NUMERICAL ANALYSIS OF COMBUSTION WAVES AND RIEMANN SOLUTIONS IN LIGHT POROUS FOAM

G. CHAPIRO[1], L. FURTADO[2], D. MARCHESIN[3], AND S. SCHECTER[4]

Abstract. In the previous work, the existence of travelling waves was proven for a system of three evolutionary parital differential equations modelling combustion of light porous foam under air injection. The wave sequences appearing in the Riemann solutions were also identified. In order to simplify the analysis, distinctions between some sequences were neglected. The analysis presented in this work leads to a re-classification and re-enumeration of the possible generic wave sequences in the solution of the combustion problem in light porous foam. We also studied numerically the hypotheses for existence of the fast combustion waves. This analysis leads to a description of a manifold in parameter space which separates different types of combustion.

1. Introduction

This paper is part of long-term research project to identify waves that arise in one-dimensional models of flow in porous media, and to understand how the waves fit together in solutions of Riemann problems; see [4, 5, 6, 12, 13, 14, 15, 18, 7], and references therein. Such flows give rise to reaction-convection-diffusion equations in which the three aspects are of roughly equal importance.

The paper performs a careful numerical analysis of waves arising in a model for the injection of air into a porous medium that contains a solid fuel. The model was proposed in [1] and further studied in [5, 6], and in [7], where it was simplified by ignoring the dependence of gas density on temperature. This simplification facilitates the study of traveling waves and the identification of the wave sequences that can occur as solutions of Riemann problems.

The model, which is reviewed in Section 2 and derived in [7], consists of three equations that express energy, oxygen, and fuel balance laws. We use a shifted Arrhenius law for which combustion begins at a threshold temperature. We analyze the case in which the thermal capacity of the medium is negligible compared to that of air. A consequence is that oxygen and heat are both transported at the velocity of the moving gas. The thermal capacity assumption is not correct for oil recovery, but is approximately valid for polyurethane foam such as that used in furniture.

In [7] four types of combustion waves were found that approach their end states exponentially, two that propagate faster than oxygen and temperature, and two that propagate more slowly. Fast combustion waves represent "premixed combustion": combustion, once it

[1] Departamento de Matemática, Universidade Federal de Juiz de Fora, Juiz de Fora, MG 36036-900, Brasil. (grigori@ice.ufjf.br)

[2] Columbia College, Columbia University, New York, NY 10027, USA. (lcf2125@columbia.edu)

[3] Instituto Nacional de Matemática Pura e Aplicada, Estrada Dona Castorina 110, Rio de Janeiro, RJ 22460-320, Brasil. (marchesi@impa.br)

[4] Mathematics Department, North Carolina State University, Raleigh, NC 27695-8205, USA. (schecter@math.ncsu.edu)

starts, races, in the form of a burning front, into a region where both solid fuel and oxygen are present. Behind the front either oxygen or fuel is exhausted. The slow combustion waves found have been called "reaction-trailing smolder waves" [19] and "coflow (or forward) filtration combustion waves" [2] in the context of more complicated models of injection of air into a porous medium. The moving gas brings oxygen into a region where solid fuel is present. The oxygen is consumed in the reaction. Since the gas velocity is greater than that of the flame front, a region of high temperature and no oxygen is swept ahead of the front. Properties of both fast and slow combustion waves are reviewed in Section 3.

As discussed in [7], for initial-boundary value problems on an infinite interval with constant boundary data, one expects the solution to resolve into combustion waves and intervals in which combustion does not occur. On these intervals the equations decouple, so one expects to observe standing solid fuel concentration patterns, convected oxygen concentration patterns, and temperature waves. Viewed from a distance, these waves resemble contact discontinuities. In Section 4 we show that only certain contact discontinuities can occur in generic wave sequences.

In Section 5 we present the generic wave sequences that could be observed for large time. For some boundary conditions, several different wave sequences are possible; they are expected to be observed for different initial data. The most complicated of the wave sequences include both a slow and a fast combustion wave. We present numerical simulations in which the expected wave sequences occur.

Since we only consider generic boundary data, we do not consider the possibility that at one end, combustion fails to occur for more than one reason. For example, we do not consider the possibility that at the right, there is both no oxygen and a low temperature. Some such boundary value problems are of course physically important, and will be the subject of future research.

Our system can be rewritten as one balance law coupled to two conservation laws, which allow reduction of the traveling wave system to two dimensions. In Section 6 we perform this reduction and study equilibria of the traveling wave system. In Sections (7) and (8) of [7] existence of the various combustion waves was proved.

2. Model

The system we consider is

$$\partial_t \theta + a\partial_x \theta = \partial_{xx}\theta + \rho Y \Phi, \tag{2.1}$$

$$\partial_t \rho = -\rho Y \Phi, \tag{2.2}$$

$$\partial_t Y + a\partial_x Y = -\rho Y \Phi, \tag{2.3}$$

$$\Phi = \begin{cases} \exp\left(-1/\theta\right), & \theta > 0 \\ 0, & \theta \leq 0. \end{cases} \tag{2.4}$$

There are three dependent dimensionless variables: temperature θ, solid fuel concentration ρ, and oxygen concentration Y. The oxygen is a component of a gas that is moving with velocity $a > 0$. Both oxygen and heat are assumed to be transported with this velocity. An exothermic chemical reaction involving oxygen and the solid fuel can occur only when the temperature is above a threshold temperature, which we normalize to be $\theta = 0$. Because of this convention, the temperature is allowed to be negative. The unit reaction rate is given as

Arrhenius law in (2.4) by $\Phi(\theta)$. Equation (2.1) represents transport and diffusion of temperature, and generation of thermal energy by the chemical reaction. Equation (2.2) represents consumption of the solid fuel, which of course does not diffuse and is not transported by the gas. Equation (2.3) represents transport of oxygen and consumption of oxygen in the chemical reaction. Diffusion of oxygen is ignored as in [1]. A derivation of the model, and discussion of its range of validity, can be found in Appendix A of [7].

We are of course interested in solutions with $\rho \geq 0$ and $Y \geq 0$ everywhere. We consider (2.1)–(2.2) on $-\infty < x < \infty$, $t \geq 0$, with the constant boundary conditions

$$(\theta, \rho, Y)(-\infty) = (\theta^L, \rho^L, Y^L), \qquad (\theta, \rho, Y)(\infty) = (\theta^R, \rho^R, Y^R). \tag{2.5}$$

As usual, we assume that the reaction does not occur at the boundaries, i.e., the reaction terms in (2.1)–(2.3) vanish. There are three reasons the reaction terms can vanish:

(1) Temperature control (TC) – reaction ceases due to low temperature $\theta \leq 0$;
(2) Fuel control (FC) – reaction ceases due to lack of fuel $\rho = 0$;
(3) Oxygen control (OC) – reaction ceases due to lack of oxygen $Y = 0$.

Of course, two or all three of these conditions can occur simultaneously. As in [7], we limit ourselves to generic boundary conditions:

(L) Exactly one of the following conditions holds: $\theta^L \leq 0$, or $\rho^L = 0$, or $Y^L = 0$. The other two numbers are positive.
(R) Exactly one of the following conditions holds: $\theta^R \leq 0$, or $\rho^R = 0$, or $Y^R = 0$. The other two numbers are positive.

3. Combustion waves

In this section we review nomenclature and some results obtained in [7]. We denote by $(\theta^-, \rho^-, Y^-) \xrightarrow{c} (\theta^+, \rho^+, Y^+)$ a wave of velocity c that connects (θ^-, ρ^-, Y^-) at the left to (θ^+, ρ^+, Y^+) at the right. At the end states of the wave, the reaction terms in (2.1)–(2.3) vanish.

States at which the reaction terms vanish were classified as TC, FC, OC, $TC \cap FC$, $TC \cap OC$, $FC \cap OC$, or $TC \cap FC \cap OC$. The type of the state indicates exactly which conditions hold at that state; for example, a $TC \cap FC$ state has $\theta \leq 0$, $\rho = 0$, and $Y > 0$. A wave of velocity c from a state of type $FC \cap OC$ to one of type TC, for example, would be indicated $FC \cap OC \xrightarrow{c} TC$. States other than TC, FC, and OC cannot be the first or last state of a wave sequence because of assumptions (L) and (R). However, as seen in [7], they cannot be ignored as possible intermediate states.

By a "combustion wave" we shall mean a continuous nontrivial traveling wave with velocity $c > 0$, $c \neq a$. We do not consider waves with velocity $c < 0$, since we have in mind injecting air into one end of a porous medium. Thus the spatial domain would be $0 \leq x < \infty$, so waves with negative velocity would not be supported. Waves with velocity $c = 0$ and $c = a$, the characteristic velocities of the system, were considered separately in [7]; we quickly review their properties.

We are concerned especially with combustion waves that approach both end states exponentially. This limitation allows us to ignore certain waves that exist only when $\theta^+ = 0$, but approach the right state more slowly than exponentially. The consequence is that we can treat right states with $\theta^+ = 0$ exactly like right states with $\theta^+ < 0$. The limitation would also allow us to ignore traveling waves with $\theta^- = 0$, since it turns out that they necessarily approach the left state more slowly than exponentially. However, in this case, the traveling

waves represent bifurcations that we find it helpful to understand. For other approaches see [1, 2, 5, 10, 19, 21].

In Theorem 3.1 of [7] it was established that there are exactly four types of combustion waves that approach both end states exponentially, two fast (wave velocity $c_f > a$) and two slow (positive wave velocity $c_s < a$): $FC \xrightarrow{c_f} TC$, $OC \xrightarrow{c_f} TC$, $FC \xrightarrow{c_s} OC$, $TC \xrightarrow{c_s} OC$.

In a fast combustion wave, the burning front moves toward a low-temperature region with both solid fuel and oxygen; this is often called "premixed combustion." The heat produced remains behind the combustion front because the moving gas that could transport it has lower velocity. Behind the front the reaction stops because the fuel is exhausted ($FC \xrightarrow{c_f} TC$), the oxygen is exhausted ($OC \xrightarrow{c_f} TC$), or both ($FC \cap OC \xrightarrow{c_f} TC$). These fronts are studied in Section (7) of [7], where the following result was proved.

Theorem 3.1. *Fast Combustion Waves. Fix $a > 0$. Let (θ^+, ρ^+, Y^+) be a state of type TC, i.e., $\theta^+ \leq 0$, $\rho^+ > 0$, $Y^+ > 0$. Assume in addition that $\theta^+ + Y^+ > 0$. Then there exists a state (θ^-, ρ^-, Y^-) and a velocity $c_f > a$ such that there is a combustion wave $(\theta^-, \rho^-, Y^-) \xrightarrow{c_f} (\theta^+, \rho^+, Y^+)$ that approaches its right state exponentially. It has $\theta^- > 0$, and ρ^- or Y^- or both equal to 0. More precisely, for fixed (θ^+, ρ^+), there is a unique Y_*^+ with $\theta^+ + Y_*^+ > 0$ such that*

(1) if $-\theta^+ < Y^+ < Y_*^+$, then there exists a combustion wave of type $OC \xrightarrow{c_f} TC$;
(2) if $Y^+ = Y_*^+$, then there exists a combustion wave of type $FC \cap OC \xrightarrow{c_f} TC$;
(3) if $Y^+ > Y_*^+$, then there exists a combustion wave of type $FC \xrightarrow{c_f} TC$.

In all cases, $\theta^+ + Y^+ = \theta^- + Y^-$ and $c_f = \frac{aY^+ - aY^-}{Y^+ - Y^- + \rho^- - \rho^+}$. In the first and third cases the wave also approaches its left state exponentially; in the second case it does not. There are no combustion waves with $c > a$ and $\theta^+ + Y^+ \leq 0$.

Theorem 3.1 says that if the right state has too little oxygen (i.e., if $\theta^+ + Y^+ \leq 0$), then the reaction cannot occur; if it has a moderate amount of oxygen, then there exists a combustion wave in which all the oxygen is used up in the reaction; and if it has lots of oxygen, then there exists a combustion wave in which all the fuel is used up in the reaction.

We conjecture that the combustion waves described in Theorem 3.1 are unique and depend smoothly on the right state, i.e., given $a > 0$, $\theta^+ \leq 0$, $\rho^+ > 0$, and $Y^+ > -\theta^+$, there is a unique $c > a$, given by a smooth function of (θ^+, ρ^+, Y^+), such that there is a combustion wave with velocity c and left state (θ^+, ρ^+, Y^+). In Section (9) of [7] we present numerical evidence for the uniqueness.

When the right state of a combustion wave is temperature-controlled, the oxygen concentration there, Y^+, is typically $\mathcal{O}(1)$. Thus the assumption $\theta^+ + Y^+ > 0$ holds whenever the temperature θ^+ at the right state is not too far below ignition temperature 0. This assumption is reasonable; in engineering it is often assumed that the two are equal.

In a slow combustion wave, a gas bringing oxygen flows into a region in which solid fuel is present but oxygen is not. Combustion occurs behind the incoming gas; it cannot occur ahead since there is no oxygen. Thus the speed of the combustion front c cannot be greater than a. In fact $c < a$, so heat produced by combustion, which also moves with speed a, is swept head of the combustion front. Hence the high-temperature region is ahead of the front. The oxygen is entirely consumed in the reaction. These fronts have been called "reaction-trailing smolder waves" [19] and "coflow (or forward) filtration combustion waves" [2]. They

were studied in Section (8) of [7], where the following results about the combustion waves were established.

Theorem 3.2. *Slow Combustion Waves.*

(1) $FC \xrightarrow{c_s} OC$ and $FC \cap TC \xrightarrow{c_s} OC$ Waves. Fix $a > 0$. Let $(\theta^-, 0, Y^-)$ have $\theta^- \geq 0$ and $Y^- > 0$. Then for each $\rho^+ > 0$, there are unique numbers $\theta^+ > 0$ and c_s, $0 < c_s < a$, such that there exists a combustion wave of velocity c_s from $(\theta^-, 0, Y^-)$ to $(\theta^+, \rho^+, 0)$. In fact,

$$\theta^+ = \theta^- + Y^-, \quad c_s = \frac{Y^-}{\rho^+ + Y^-} a. \tag{3.1}$$

These waves approach their right state exponentially, and approach their left state exponentially if and only if $\theta^- > 0$, i.e., if and only if the left state is of type FC.

(2) $TC \xrightarrow{c_s} OC$ Waves. Fix $a > 0$. Let $\theta^- < 0$, Y^- with $\theta^- + Y^- > 0$, and $\rho^+ > 0$ be given. Then there are numbers $\rho^- > 0$, $\theta^+ > 0$, and c_s, $0 < c_s < a$, such that there exists a combustion wave of velocity c_s from (θ^-, ρ^-, Y^-) to $(\theta^+, \rho^+, 0)$. Moreover $\theta^+ = \theta^- + Y^-$, and the quantities c_s and ρ^- are related by the formula

$$c_s = \frac{aY^-}{Y^- - \rho^- + \rho^+}.$$

These waves approach both end states exponentially.

(3) There are no other combustion waves $0 < c < a$. In particular, there are no slow combustion waves with $\theta^- + Y^- \leq 0$.

Theorem 3.2 (1) says that for each left state of type FC, and for the left state $(0, 0, Y^-)$ with $Y^- > 0$, there is a one-parameter family of right states of type OC to which the left state can be connected by a slow combustion wave.

On the other hand, Theorem 3.2 (2) says that to have a slow combustion wave of speed c_s from a left state (θ^-, ρ^-, Y^-) of type TC to a right state $(\theta^+, \rho^+, 0)$ of type OC, the triple (θ^-, Y^-, ρ^+) may be chosen arbitrarily, and then a corresponding triple (ρ^-, θ^+, c_s) can be found. Section (9) of [7] presents numerical evidence that the triple (ρ^-, θ^+, c_s) is unique.

The set of points in $(\theta^-, \rho^-, Y^-, \theta^+, \rho^+, c_s)$-space that corresponds to $TC \xrightarrow{c_s} OC$ waves should be a three-dimensional manifold. We have not shown this, but if it is true, then by Sard's Theorem, almost every left state corresponds to a set of isolated right states (which may be empty). We conjecture that in fact every left state corresponds to a unique right state.

4. Contact discontinuities

In the absence of reaction and diffusion terms, the characteristic velocities of (2.1)–(2.3) are 0 for the solid fuel and a for temperature and oxygen. Contact discontinuity waves therefore have velocity 0 or a. The solid fuel concentration can change across a contact discontinuity of velocity 0, while temperature or oxygen concentration or both can change across a contact discontinuity of velocity a. Contact discontinuities must separate intervals on which the reaction does not occur (since (θ, ρ, Y) is constant).

The waves must occur in order of increasing velocity. It is easy to see that there is at most one slow combustion wave and one fast combustion waves. We may also assume:

(O) There is at most one wave of velocity 0 and one of velocity a.

The reason is that a sequence of two contact discontinuities with the same velocity could be combined into one.

The *dimension number* of a contact discontinuity is the dimension of the set of right states that can be reached from a fixed left state by a contact discontinuity of the given type. For example, for a contact discontinuity of speed 0, the ρ-component of the right state can be varied (dimension 1) unless it is 0 (dimension 0). For a contact discontinuity of speed a, both the the θ- and Y-components of the right state can be varied (dimension 2), unless the Y-component of the right state is 0 (dimension 1). The following was proven in [7]:

Theorem 4.1. *With assumptions (L), (R), and (O), the contact discontinuities that occur in generic wave sequences are those given in Table 4.1.*

TABLE 4.1. Contact discontinuities

Contact discontinuity	Dimension number
$TC \xrightarrow{0} TC$	1
$TC \xrightarrow{0} TC \cap FC$	0
$OC \xrightarrow{0} OC$	1
$OC \xrightarrow{0} FC \cap OC$	0
$TC \xrightarrow{a} TC$	2
$TC \xrightarrow{a} OC$	1
$FC \xrightarrow{a} FC$	2
$OC \xrightarrow{a} OC$	1
$OC \xrightarrow{a} TC$	2
$TC \cap FC \xrightarrow{a} FC$	2
$FC \cap OC \xrightarrow{a} FC$	2

We remark that four of the these contact discontinuities begin or end at states of type $TC \cap FC$ or $OC \cap FC$. By assumptions (L) and (R), these states cannot be the first or last in the wave sequence. They can, however, be intermediate states in generic wave sequences. In the paper, it was shown that contact discontinuities other than the given types cannot occur in generic wave sequences.

As shown in the paper, there remain fifteen possible contact discontinuities of speed a: five possible left states (TC, FC, OC, $TC \cap FC$, $FC \cap OC$) and three possible right states (TC, FC, OC). Eight cannot occur because a wave of speed a cannot remove or create the condition FC: $FC \xrightarrow{a} TC$, $FC \xrightarrow{a} OC$, $TC \cap FC \xrightarrow{a} TC$, $TC \cap FC \xrightarrow{a} OC$, $FC \cap OC \xrightarrow{a} TC$, $FC \cap OC \xrightarrow{a} OC$, $TC \xrightarrow{a} FC$, $TC \xrightarrow{a} OC$. The remaining seven are listed in the table.

5. Wave Sequences

Table 5.1 lists the four types of combustion waves in Theorem 3.1 of [7], together with their dimension numbers, which were explained in Section 3.

An obvious necessary condition for a wave sequence to be generic is that it begins at a state S^L of type TC, FC, or OC, and ends at a state S^R of type TC, FC, or OC. If S^R is of type FC ($\rho^R = 0$), there is a two-parameter family of states of the same type nearby obtained by varying θ^R and Y^R. Similarly, if S^R is of type OC, there is a two-parameter family of states of the same type nearby obtained by varying θ^R and ρ^R; and if S^R is of type

TABLE 5.1. Combustion waves

Combustion wave	Dimension number
$FC \xrightarrow{c_f} TC$	1
$OC \xrightarrow{c_f} TC$	1
$FC \xrightarrow{c_s} OC$	1
$TC \xrightarrow{c_s} OC$	0

TC, there is a three-parameter family of states of the same type nearby, since θ^R can be varied along with ρ^R and Y^R.

Thus a second necessary condition for a wave sequence from a left state S^L to a right state S^R to be generic is that for left states of the same type near S^L, the intermediate states of the wave sequence can be varied to arrive at

- a two-parameter family of states near S^R if S^R is of type FC or OC;
- a three-parameter family of states near S^R if S^R is of type TC.

It follows that for a wave sequence to be generic, the wave dimension numbers must sum to at least 2 if the right state is of type FC or OC, and to at least 3 if the right state is of type TC.

Figure 5.1 shows all possible sequences of the waves in Theorems 3.1 [7] and 4.1 with (1) left state of type TC, FC, or OC, (2) increasing wave speed, and (3) sequences extended as far as possible. Wave dimension numbers are also indicated. From this figure one can read off all wave sequences with (1) left state of type TC, FC, or OC, (2) right state of type TC, FC, or OC, and (3) correct sum of the wave numbers. These 18 sequences are listed below; by giving the intermediate states explicitly we verify that they are in fact generic. Generic wave sequences ending at states of type FC or OC (respectively TC) all have dimension number sum 2 (respectively 3). Wave sequences with higher dimension number sum do not exist.

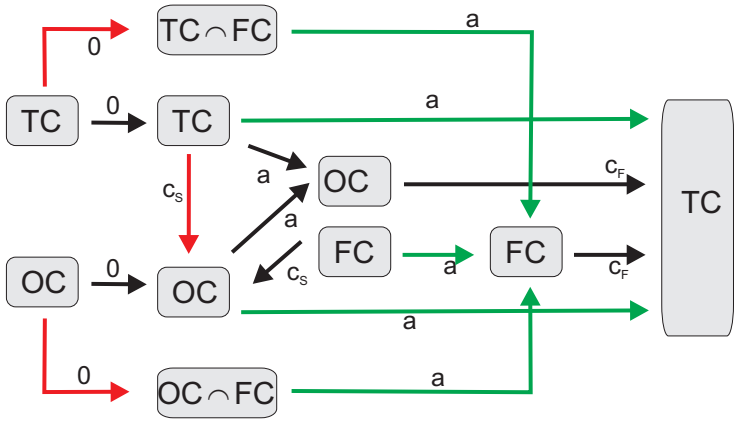

FIGURE 5.1. All possible sequences of the waves in Tables 4.1 and 5.1 with (1) left state of type TC, FC, or OC, (2) increasing wave speed, and (3) sequences extended as far as possible. Red arrow: dimension number 0. Black arrow: dimension number 1. Green arrow: dimension number 2.

There are nine types of boundary value problems, depending on whether the left and right states are temperature controlled (TC), fuel controlled (FC), or oxygen controlled (OC). We first give a brief summary the possible wave sequences, followed by a detailed account for the interested reader.

1. Fuel-controlled right state. A combustion wave moving right cannot occur because there is no fuel at the right and no mechanism to bring fuel to the right. Each possible left state gives rise to a unique sequence of contact discontinuities. Notice that this wave sequence represents the asymptotic state of the system. Combustion may occur for a while in certain regions (for example, regions where fuel, oxygen, and high temperature are initially present), but it eventually stops.

2. Oxygen-controlled right state. Each possible left state again gives rise to a unique sequence of contact discontinuities, in which there are no combustion waves. In addition, fuel-controlled and temperature controlled left states allow a wave sequence with a slow combustion wave (smoldering). When there is an oxygen-controlled right state, combustion must eventually die out unless oxygen is constantly brought to the right; this can only happen when the left state has a positive oxygen concentration.

3. Temperature-controlled right state. Again each possible left state again gives rise to a unique sequence of contact discontinuities, in which there are no combustion waves. In addition, there is a rich set of other possibilities.

- Each possible left state allows a wave sequence consisting of one or two contact discontinuities followed by a fast combustion wave. This is not surprising: the right state is "premixed," in that both oxygen and fuel are present. If combustion starts anywhere in the premixed region (because, for example, a high temperature is initially present there), then the combustion process itself produces a wave of high temperature moving further into the premixed.
- A temperature-controlled left state allows a wave sequence in which there is a single slow combustion wave surrounded by contact discontinuities. The oxygen arriving from the left leads to a slow combustion wave preceded by a region of no oxygen: the oxygen arriving from the left all burned in the reaction, and the oxygen initially present at the right is carried away before the flame can reach it. Thus we have smoldering despite a premixed right state.
- Finally, temperature-controlled and oxygen-controlled left states each allow a wave sequence that includes both a slow and a fast combustion wave.

6. Reduced traveling wave equation

In order to most conveniently find the combustion waves of the system (2.1)–(2.3), we replace (2.2) by the sum of (2.2) and (2.1), and we replace (2.3) by the difference of (2.3) and (2.2). We obtain

$$\partial_t \theta + a\partial_x \theta = \partial_{xx}\theta + \rho Y \Phi(\theta), \tag{6.1}$$

$$\partial_t(\theta + \rho) + a\partial_x \theta = \partial_{xx}\theta, \tag{6.2}$$

$$\partial_t(Y - \rho) + a\partial_x Y = 0. \tag{6.3}$$

In (6.1)–(6.3), we replace the spatial coordinate x with one ξ that is moving with velocity c: $\xi = x - ct$. To obtain the stationary solutions, we neglect $\frac{d}{dt}$ terms .....

In (**??**), we set $v_1 = \partial_\xi \theta$, and we integrate (**??**)–(**??**). Using dot to denote derivative with respect to ξ, we obtain the system

$$\dot{\theta} = v_1, \tag{6.4}$$
$$\dot{v}_1 = (a-c)v_1 - \rho Y \Phi(\theta), \tag{6.5}$$
$$w_1 = (c-a)\theta + v_1 + c\rho, \tag{6.6}$$
$$w_2 = (c-a)Y - c\rho, \tag{6.7}$$

where w_1 and w_2 are constants.

We assume $c \neq a$. Then we can solve for Y using (6.7), and we solve for v_1 using (6.6). Substituting into (6.4)–(6.5) and dividing the second equation by c (we recall the standing assumption hat $c > 0$), we obtain the reduced traveling wave system

$$\dot{\theta} = (a-c)\theta - c\rho + w_1, \tag{6.8}$$
$$\dot{\rho} = \frac{c\rho + w_2}{c(c-a)} \rho \Phi(\theta), \tag{6.9}$$

in which (w_1, w_2) is a vector of parameters. Because of (6.7), for the system (6.8)–(6.9),

$$\text{the point } (\theta, \rho) \text{ has } Y = \frac{c\rho + w_2}{c-a}. \tag{6.10}$$

The system (6.8)–(6.9) has the invariant lines

$$\rho = 0 \quad \text{and} \quad \rho = -\frac{w_2}{c};$$

the latter corresponds to $Y = 0$.

The physically relevant part of the phase space for (6.8)–(6.9), which we denote P, has $\rho \geq 0$ and $Y \geq 0$. From (6.10),

$$\text{if } 0 < c < a,\ Y \geq 0 \text{ if and only if } \rho \leq -\tfrac{w_2}{c}; \tag{6.11}$$
$$\text{if } c > a,\ Y \geq 0 \text{ if and only if } \rho \geq -\tfrac{w_2}{c}. \tag{6.12}$$

In the first case, P is nonempty if $w_2 \leq 0$; $P = \{(\theta, \rho) : 0 \leq \rho \leq -\frac{w_2}{c}\}$. In the second case, $P = \{(\theta, \rho) : \rho \geq \max(0, -\frac{w_2}{c})\}$. In both cases P is invariant.

6.1. **Equilibria.** The set of equilibria of (6.8)–(6.9) is the union of three subsets:

$$FC = \{(\theta, \rho) : \theta > 0,\ \rho = 0,\ c\rho + w_2 > 0,\ \text{and } (a-c)\theta - c\rho + w_1 = 0\},$$
$$OC = \{(\theta, \rho) : \theta > 0,\ \rho > 0,\ c\rho + w_2 = 0,\ \text{and } (a-c)\theta - c\rho + w_1 = 0\},$$
$$FC \cap OC = \{(\theta, \rho) : \theta > 0,\ \rho = 0,\ c\rho + w_2 = 0,\ \text{and } (a-c)\theta - c\rho + w_1 = 0\}.$$
$$TC^* = \{(\theta, \rho) : \theta \leq 0 \text{ and } (a-c)\theta - c\rho + w_1 = 0\}.$$

FC, OC, and $FC \cap OC$ consist of equilibria of those types only (recall (6.10)). TC^* includes equilibria of types TC, $TC \cap FC$, $TC \cap OC$, and $TC \cap FC \cap OC$, i.e., all low-temperature equilibria.

All equilibria lie on the line H defined by $(a-c)\theta - c\rho + w_1 = 0$. H has positive slope if $0 < c < a$ and negative slope if $c > a$. In terms of the natural variables (θ, v_1, ρ, Y), with $v_1 = \dot{\theta}$, H corresponds to $v_1 = 0$. The portion of H in $\theta \leq 0$ is TC; the portion in $\theta > 0$ is the disjoint union of FC ($\rho = 0$ only), OC ($Y = 0$ only), and $FC \cap OC$ ($\rho = Y = 0$).

The linearization of (6.8)–(6.9) at a point (θ, ρ) has the matrix

$$\begin{pmatrix} a-c & -c \\ \dfrac{c\rho + w_2}{c(c-a)}\rho\Phi'(\theta) & \dfrac{2c\rho + w_2}{c(c-a)}\Phi(\theta) \end{pmatrix}. \tag{6.13}$$

If $(\theta, \rho) \in TC^*$, (6.13) becomes

$$\begin{pmatrix} a-c & -c \\ 0 & 0 \end{pmatrix}. \tag{6.14}$$

Proposition 6.1. *At an equilibrium in TC^*, one eigenvalue is $a-c$, with eigenvector $(1,0)$; the other eigenvalue is 0.*

If $(\theta, \rho) \in FC$ or $FC \cap OC$, (6.13) becomes

$$\begin{pmatrix} a-c & -c \\ 0 & \dfrac{w_2}{c(c-a)}\Phi(\theta) \end{pmatrix}. \tag{6.15}$$

We have $\rho = 0$. In FC, $Y > 0$, so

$$w_2 = (c-a)Y - c\rho = (c-a)Y \text{ has the sign of } c-a.$$

In $FC \cap OC$, $Y = 0$, so $w_2 = 0$. Therefore:

Proposition 6.2. *At an equilibrium in FC or $FC \cap OC$, one eigenvalue is $a-c$, with eigenvector $(1,0)$. This eigenvector points along the invariant line $\rho = 0$. The other eigenvalue is positive in FC and 0 in $FC \cap OC$. Its eigenvector is transverse to the invariant line.*

If $(\theta, \rho) \in OC$, (6.13) becomes

$$\begin{pmatrix} a-c & -c \\ 0 & \dfrac{w_2}{c(a-c)}\Phi(\theta) \end{pmatrix}. \tag{6.16}$$

Since $\rho > 0$ and $c\rho + w_2 = 0$, we have $w_2 < 0$. Therefore:

Proposition 6.3. *An equilibrium in OC is a saddle. One eigenvalue is $a-c$, with eigenvector $(1,0)$. This eigenvector points along the invariant line $\rho = -w_2/c$, which corresponds to $Y = 0$. The other eigenvector is transverse to the invariant line.*

The invariant lines $\rho = -\frac{w_2}{c}$ and $\rho = 0$ each contain just one equilibrium, so they do not contain traveling waves with finite limits at both ends. Therefore, from the propositions of this section we conclude that to find solutions of (6.8)–(6.9) that approach their end states exponentially, only the following cases need be considered:

- $0 < a < c$, left state in FC or OC, right state in TC^*.
- $0 < c < a$, left state in FC or TC^*, right state in OC.

7. Numerically determining the wave sequences

In this section, we describe a way to numerically determine a (θ^-, ρ^-, Y^-) and c_f, given (θ^+, ρ^+, Y^+) in accordance with the hypotheses of Theorem 3.1. The method, which was implemented in MATLAB, begins by determining the type of combustion wave that will occur, for specified (θ^+, ρ^+, Y^+). By Theorem 3.1, the problem of determining the type of combustion wave translates to that of finding the value of Y_*^+ for each (θ^+, ρ^+, a). The next section describes the procedure by which this was done.

7.1. **Finding Y_*^+ Numerically and a Numerical Analysis Thereof.** Assume $\rho^- = Y^- = 0$ so that $\theta^- = \theta^+ + Y^+$ and the left state is of type $FC \cap OC$, in which case $Y_*^+ = Y^+$ and $c_f = aY^+/(Y^+ - \rho^+)$. For a given fixed (θ^+, ρ^+, a), look for a value of Y^+ that will give a combustion wave from the left state (which in this case is $FC \cap OC$ and unique and of the form $(\theta^-, \rho^-, Y^-) = (\theta^+ + Y^+, 0, 0)$) to the right state (θ^+, ρ^+, Y^+).

Specifically, for each given value of $(\theta^+, \rho^+, Y^+, a)$, substitute into (6.8)–(6.9) the values

$$w_1 = (a-c)\theta^+ + c\rho^+, \quad w_2 = (c-a)Y^+ - c\rho^+, \quad c = c_f = aY^+/(Y^+ - \rho^+). \tag{7.1}$$

Then define

$$\psi_{(\theta^+,\rho^+,Y^+)} : t \in \mathbb{R} \mapsto (\theta(t), \rho(t)) \in \mathbb{R}^2 \tag{7.2}$$

to be the solution of (6.8)–(6.9) (with w_1, w_2, and c as already mentioned) whose α-limit is the equilibrium point $FC \cap OC$ described in Section 6.1.

The integration is done numerically— it is possible to only approximately find this orbit. This approximation is done by linearizing (6.8)–(6.9), (see matrix (6.13)) and plotting an orbit beginning a short distance from the equilibrium point $FC \cap OC$, in the direction of the eigenvector corresponding to the eigenvalue $\lambda = 0$ (the other eigenvector is negative: see Proposition 6.1).

Let $\tilde{t} \in \mathbb{R}$ be the time such that

$$\psi_{(\theta^+,\rho^+,Y^+)}(\tilde{t}) = (0, \tilde{\rho}), \tag{7.3}$$

i.e., the time when the orbit crosses the ρ-axis. Finally, define F_{θ^+,ρ^+} as the function that takes

$$Y^+ \mapsto (\rho^+ - \psi_{(\theta^+,\rho^+,Y^+)}(\tilde{\rho})) = \rho^+ - \tilde{\rho}. \tag{7.4}$$

Then Y_*^+ is a zero of F_{θ^+,ρ^+}, namely,

$$F_{\theta^+,\rho^+}(Y_*^+) = \rho^+ - \psi_{(\theta^+,\rho^+,Y_*^+)}(\tilde{\rho}) = \rho^+ - \tilde{\rho} = 0 \tag{7.5}$$

because Y_*^+ is defined to be the value of Y^+ for which there is a combustion wave $(\theta^-, \rho^-, Y^-) = (\frac{-w_1}{a-c}, 0, 0) \xrightarrow{c_f} (\theta^+, \rho^+, Y^+)$ of type $FC \cap OC \xrightarrow{c_f} TC$. In other words, Y_*^+ is the value of Y^+ for which there exists an orbit of (6.8)-(6.9) with α-limit (θ^-, ρ^-, Y^-) and ω-limit (θ^+, ρ^+, Y^+), so that

$$\psi_{(\theta^+,\rho^+,Y_*^+)}(\tilde{\rho}) = \psi_{(\theta^+,\rho^+,Y_*^+)}(+\infty) = \rho^+. \tag{7.6}$$

Note that the first equality holds because for values of $\theta \leq 0$, $\dot{\rho}$ vanishes in (6.9). This is why we may stop the numerical integration of (6.8)-(6.9) at $\theta = 0$, without having to go further for values of $\theta < 0$. Lastly, the method of bisection was used to find the zero of F_{θ^+,ρ^+}.

7.2. **Numerical Analysis of the Relationship Between Y_*^+ and (θ^+, ρ^+, a).** Using the procedure described above, we found and plotted in (θ^+, ρ^+, Y^+)-space the corresponding value of $Y_*^+(\theta^+, \rho^+, a)$. Here we consider Y_*^+ as a function of (θ^+, ρ^+, a), for various values of (θ^+, ρ^+, a).

Fixed a, the graph of the function Y_*^+ is a 2-dimensional level-surface in (θ^+, ρ^+, Y^+)-space (see Figure 7.1). We found that these level surfaces do not intersect on the interval $(-10, 0.2, 0.1) \leq (\theta^+, \rho^+, Y_*^+) \leq (-0.2, 10, 10)$. They do appear to intersect in the limit $\rho^+ \to 0$ (see Figure 7.2). Furthermore, for $0.1 \leq a \leq 10$, as $\rho^+ \to 0$ it appears that $Y_+^* \to \theta^+$. For very large values of a however either this does not appear to be the case, or $Y_+^* \to \theta^+$ so slowly that the simulation is not capable to distinguish sufficiently small values of $\rho^+ > 0$.

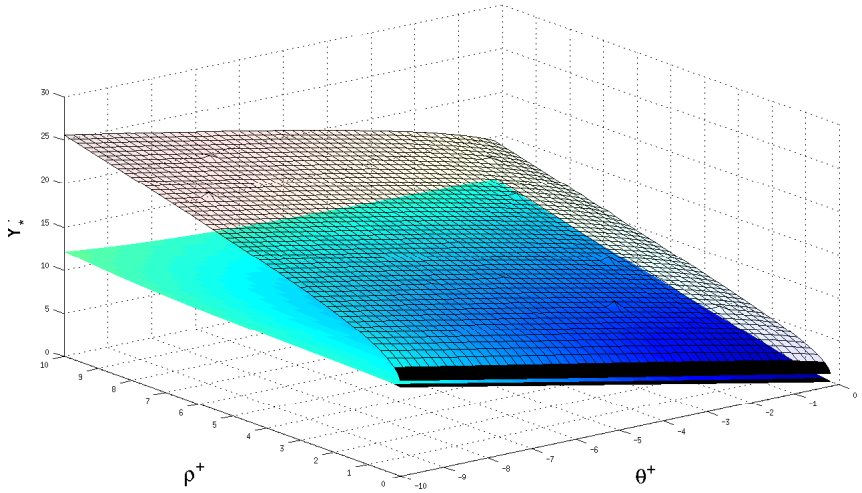

FIGURE 7.1. The graph of $Y_*^+(\theta^+, \rho^+, a)$ for a = 0.1 (below) and a = 4 (above).

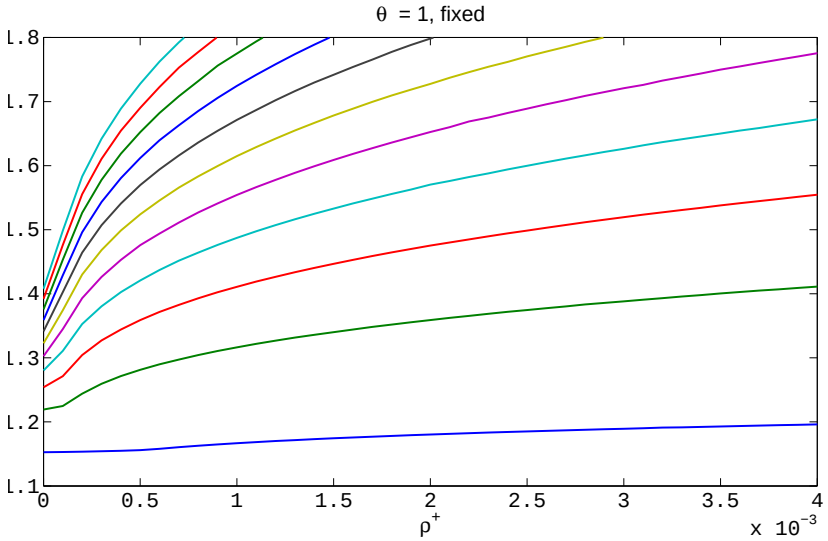

FIGURE 7.2. For fixed θ^+ and ρ^+ small. The curves, from bottom to top, have increasing values of a equal to 0.1, 1, 2, 3, 4, 5, 6, 7, 8, 9, and 10.

8. Numerical Stability of Wave Sequences

In this section we study the stability of the generic sequences discussed in [7].

Theorem 3.2 states that if $\theta^- + Y^- < 0$, then slow combustion will not exist; Theorem 3.1 states that if $\theta^+ + Y^+ < 0$, then fast combustion will not exist. When an end state is of type $TC^>$, combustion waves arriving at or coming from temperature controlled regions may occur, by Theorems 3.1 and 3.2. Therefore, we distinguish states of type TC according to whether they do or do not fit these conditions. We subdivide TC into two subsets:

$$TC^{>} = \{(\theta, \rho, Y) \in TC : \ \theta + Y > 0\}, \qquad TC^{<} = \{(\theta, \rho, Y) \in TC : \ \theta + Y \leq 0\},$$

and continue writing TC to mean the union of $TC^{<}$ and $TC^{>}$.

There are 9 combinations of left and right states. We denote such a combination by an ordered pair (S^L, S^R), where S^L and S^R are 2 or 3 dimensional vectors corresponding to left and right boundary states of either type FC, OC, or TC.

Referring to the results of [7], which are summarized in Section 5, we notice that 5 of these pairs have unique wave sequences connecting their left and right boundary states:

(1) (FC, FC): $FC \xrightarrow{a} FC$
(2) (TC, FC): $TC \xrightarrow{0} TC \cap FC \xrightarrow{a} FC$
(3) (OC, FC): $OC \xrightarrow{0} OC \cap FC \xrightarrow{a} FC$
(4) (OC, OC): $OC \xrightarrow{0} OC \xrightarrow{a} OC$
(5) (FC, OC): $FC \xrightarrow{c_s} OC \xrightarrow{a} OC$

Sequences (1)-(5) either do not contain combustion waves or contain only slow combustion waves of type $FC \xrightarrow{c_s} OC$. These sequences may be computed explicitly, as described in Section 3. Simulations indicated that sequences (1)-(5) are indeed stable.

The remaining 4 pairs of end states give rise to the 13 other generic wave sequences described in [7]. Specifically, the pair (TC, OC) gives rise to 2 wave sequences, (6)-(7); (FC, TC) and (OC, TC) each give rise to wave sequences (8)-(10) and (11)-(13); and (TC, TC) gives rise to 5 wave sequences, (14)-(18). The remainder of this section is dedicated to the study of the stability of these 13 sequences, which we subdivide into 21 subsequences, listed below:

(6.1) $TC^{>} \xrightarrow{0} TC^{>} \xrightarrow{a} OC$
(6.2) $TC^{<} \xrightarrow{0} TC^{<} \xrightarrow{a} OC$
(7) $TC^{>} \xrightarrow{0} TC^{>} \xrightarrow{c_s} OC \xrightarrow{a} OC$

(8.1) $FC \xrightarrow{c_s} OC \xrightarrow{a} TC^{>}$, $Y^R > Y^*$
(8.2) $FC \xrightarrow{c_s} OC \xrightarrow{a} TC^{>}$, $Y^R < Y^*$
(8.3) $FC \xrightarrow{c_s} OC \xrightarrow{a} TC^{<}$
(9) $FC \xrightarrow{a} FC \xrightarrow{c_f} TC^{>}$
(10) $FC \xrightarrow{c_s} OC \xrightarrow{a} OC \xrightarrow{c_f} TC^{>}$

(11.1) $OC \xrightarrow{0} OC \xrightarrow{a} TC^{>}$, $Y^+ > Y^*$
(11.2) $OC \xrightarrow{0} OC \xrightarrow{a} TC^{>}$, $Y^+ < Y^*$
(11.3) $OC \xrightarrow{0} OC \xrightarrow{a} TC^{<}$
(12) $OC \xrightarrow{0} OC \cap FC \xrightarrow{a} FC \xrightarrow{c_f} TC$
(13) $OC \xrightarrow{0} OC \xrightarrow{a} OC \xrightarrow{c_f} TC$

(14) $TC \xrightarrow{0} TC \xrightarrow{a} TC$
(15.1) $TC^{>} \xrightarrow{0} TC^{>} \xrightarrow{c_s} OC \xrightarrow{a} TC^{<}$
(15.2) $TC^{>} \xrightarrow{0} TC^{>} \xrightarrow{c_s} OC \xrightarrow{a} TC^{>}$
(16.1) $TC^{<} \xrightarrow{0} TC^{<} \xrightarrow{a} OC \xrightarrow{c_f} TC^{>}$
(16.2) $TC^{>} \xrightarrow{0} TC^{>} \xrightarrow{a} OC \xrightarrow{c_f} TC^{>}$
(17.1) $TC^{<} \xrightarrow{0} TC^{<} \cap FC \xrightarrow{a} FC \xrightarrow{c_f} TC^{>}$
(17.2) $TC^{>} \xrightarrow{0} TC^{>} \cap FC \xrightarrow{a} FC \xrightarrow{c_f} TC^{>}$
(18) $TC^{>} \xrightarrow{0} TC^{>} \xrightarrow{c_s} OC \xrightarrow{a} OC \xrightarrow{c_f} TC^{>}$

In what follows, the speed of the contact discontinuity was always taken to be $a = 0.1$.

8.1. **Sequences with boundary conditions** (TC, OC).

8.1.1. $S^L \in TC^{<}$. Combustion of type $TC^{<} \xrightarrow{c_s} OC$ will not occur, by Theorem 3.2. Indeed, it was verified by the simulations that the sequence (6.2) connecting $(TC^{<}, OC)$ is indeed stable.

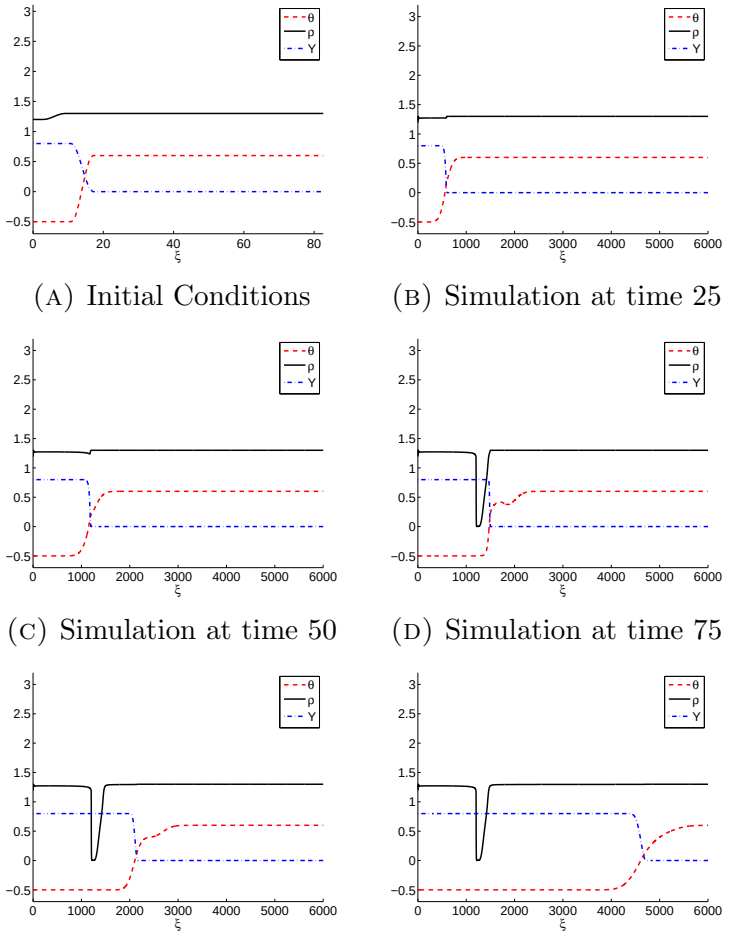

(A) Initial Conditions (B) Simulation at time 25

(C) Simulation at time 50 (D) Simulation at time 75

(E) Simulation at time 100 (F) Simulation at time 200

FIGURE 8.1. Sequence (7); Behavior 1

8.1.2. $S^L \in TC^>$. When $S^L \in TC^>$, slow combustion of type $TC^> \xrightarrow{c_s} OC$ is shown to exist by Theorem 3.2. For the pair $(TC^>, OC)$ it is possible to construct, in addition to a sequence of type (6.1), a sequence of type (7), using the numerical procedure described in Section 7. Different behaviors were observed, which depended on the end states given. The behavior also seems to depend on the distance between the waves of the given wave sequence. Namely, in the simulations performed, sequences (6.1) and (7) with the same end states always evolved into the same sequence but sequences with different end states evolved into different sequences. Hence we will explain the behavior when a sequence of type (6.1) is given as the initial condition, noting that the same behavior occurs when a sequence with the same end states of type (7) is given as the initial condition.

Three different behaviors were observed during intermediate times which in turn converge into two apparently stable sequences. The intermediate behaviors are:

(1) The initial condition quickly evolves into a sequence of type (7); a slow combustion wave of type $TC^> \xrightarrow{c_s} OC$ forms that burns increasing amounts of fuel until a time when the temperature becomes high enough, giving rise to a violent combustion that

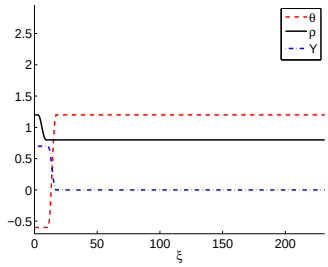

(A) Initial Conditions

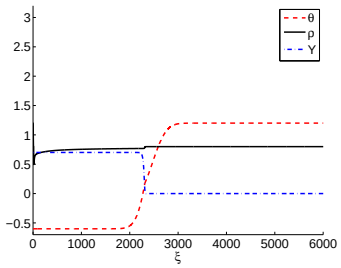

(B) Simulation at time 100

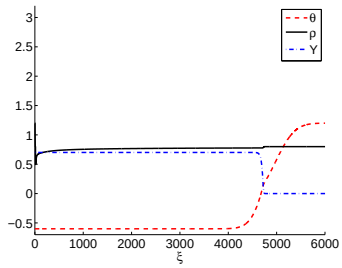

(C) Simulation at time 200

FIGURE 8.2. Sequence (7); Behavior 2

burns all of the fuel but extinguishes shortly afterwards, becoming a sequence of type (6.1) (see plots in Figure 8.1).

(2) The initial condition quickly evolves into a sequence of type (7) that burns in increasing amounts in a manner similar to behavior (1). The violent combustion does not burn all of the fuel and instead of quickly extinguishing evolves into a milder combustion that appears to be stable (or very slowly extinguishing itself) (see plots in Figure 8.2).

(3) The initial condition quickly evolves into a sequence of type (7) in a manner similar to behavior (1), eventually giving rise to a violent combustion that burns all of the fuel. Instead of extinguishing itself as in (1), this combustion continues, and appears to be stable (see plots in Figure 8.3).

Behavior (1) suggests that for certain end states slow combustion of type $TC^{>} \xrightarrow{c_s} OC$ is unstable. However, during intermediate times, slow combustion is present in behaviors (1)-(3). Although behavior (2) displays left and right states for which an apparently persistent slow combustion occurs, whether this combustion is stable or very slowly extinguishing is unclear through the simulation. Behavior (3) suggests that slow combustion of type $TC^{>} \xrightarrow{c_s} OC$ can also be stable, for certain boundary states. Theorem 3.2 proves the existence of slow combustion when $S^L \in TC^{>}$; these simulations suggest that this combustion may be unstable or stable, if in fact behavior (2) displays a stable slow combustion wave. Behavior (3), in which a slow combustion appears that burns all of the fuel, is an example of a stable sequence of type $TC \xrightarrow{0} TC \cap FC \xrightarrow{c_s} OC \xrightarrow{a} OC$. This sequence does not appear as one of the 18 possibe generic wave sequences described in Figure 5.1. Simulation (3) is evidence that this sequence is physically present. Finally, while only end states with exactly one control condition was considered, it might be beneficial to in addition consider those end

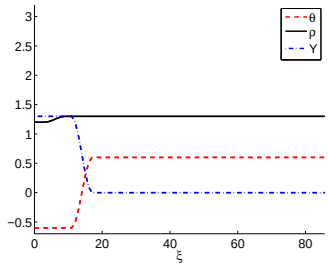

(A) Initial Conditions

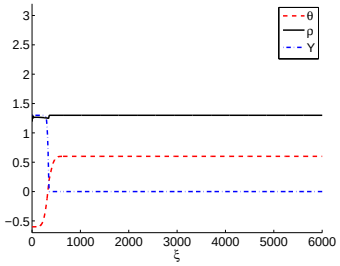

(B) Simulation at time 15

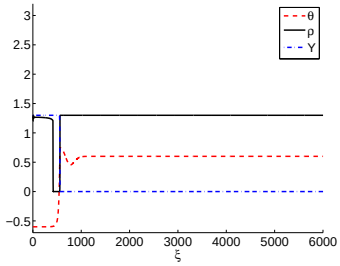

(C) Simulation at time 30

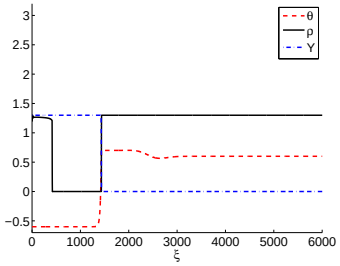

(D) Simulation at time 100

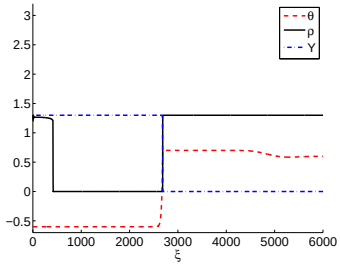

(E) Simulation at time 200

FIGURE 8.3. Sequence (7); Behavior 3

states that are both TC and either OC or FC. This is because the subsets $TC \cap OC$ and $TC \cap FC$ both have codimension 1 in (θ, ρ, Y)-space, and so should be considered generic.

8.2. **Sequences with boundary conditions** (FC, TC).

8.2.1. $S^R \in TC^<$. Fast combustion will not occur, by Theorem 3.1. It was verified by the simulations that the sequence (8.3) connecting $(FC, TC^<)$ is indeed stable.

8.2.2. $S^R \in TC^>$. Theorem 3.1 shows that fast combustion exists. The Theorem also distinguishes two types of generic fast combustion waves: $OC \xrightarrow{c_f} TC^>$ and $FC \xrightarrow{c_f} TC^>$. As stated in Theorem 3.1, the type of wave is determined by the values of the right state. Specifically, for $Y^+ > Y^*(\theta^+, \rho^+)$ the fast combustion wave is of type $FC \xrightarrow{c_f} TC$ and for $Y^+ < Y^*(\theta^+, \rho^+)$ it is of type $OC \xrightarrow{c_f} TC^>$. Recall that we described how to determine numerically the type of fast combustion wave in Section 7.

When $Y^+ > Y^*$, simulations with initial data without combustion (sequence (8.1)) quickly evolved into sequence (9) (see Figure 8.4). This is an indication that when $Y^+ > Y^*$, fast

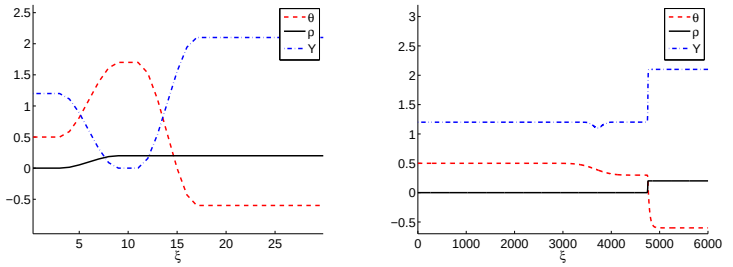

(A) Initial Conditions (B) Simulation at time 150

FIGURE 8.4. Sequence 8.1

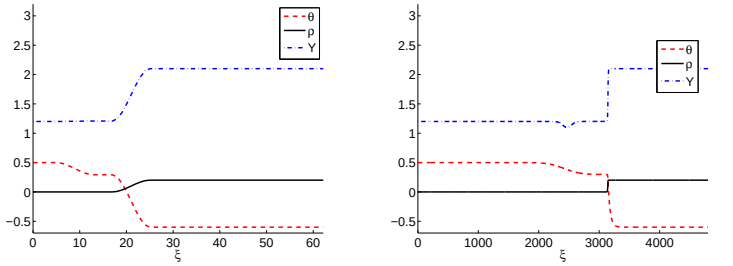

(A) Initial Conditions (B) Simulation at time 100

FIGURE 8.5. Sequence 9

combustion of type $FC \xrightarrow{c_f} TC^{>}$ exists and is stable. In fact, the simulations suggest that when $Y^+ > Y^*$, among (8.1) and (9), the latter is the only stable sequence.

When $Y^+ < Y^*$, different behaviors were observed, which suggest that both sequences, (8.2) and (10), may be stable for large time. Similar to Subsection 8.1.2, for the simulations performed the different behaviors depended on the given end states but not on the type of sequence given as initial condition. Hence, we will explain the behavior when a sequence of type (8.2) is given as initial condition, noting that the same behavior occurs when a sequence with the same boundary states of type (10) is given as the initial condition. Two different behaviors were observed during intermediate times, which in turn converge to two apparently stable sequences. These behaviors are:

(1) Periodic violent bursts of fast combustion occur; the period of the combustion increases over time. In the time intervals between the bursts of combustion, the sequence has a small fast combustion wave that decreases in magnitude before slowly increasing again in magnitude until the combustion burst (Figures 8.6 and 8.7).
(2) The initial conditions quickly evolve into a stable sequence of type (10) (Figure 8.8).

8.3. **Sequences with boundary conditions** (OC, TC)**.**

8.3.1. $S^R \in TC^{<}$. The hypotheses of Theorem 3.1 are not satisfied, so that fast combustion will not occur. It was verified by the simulations that the sequence (11.3) connecting $(OC, TC^{<})$ is indeed stable.

8.3.2. $S^R \in TC^{>}$. When $Y^+ > Y^*$, simulations with initial data without fast combustion (sequence (11.1)) quickly evolved into sequence (9) (Figure 8.13). Simulations with initial

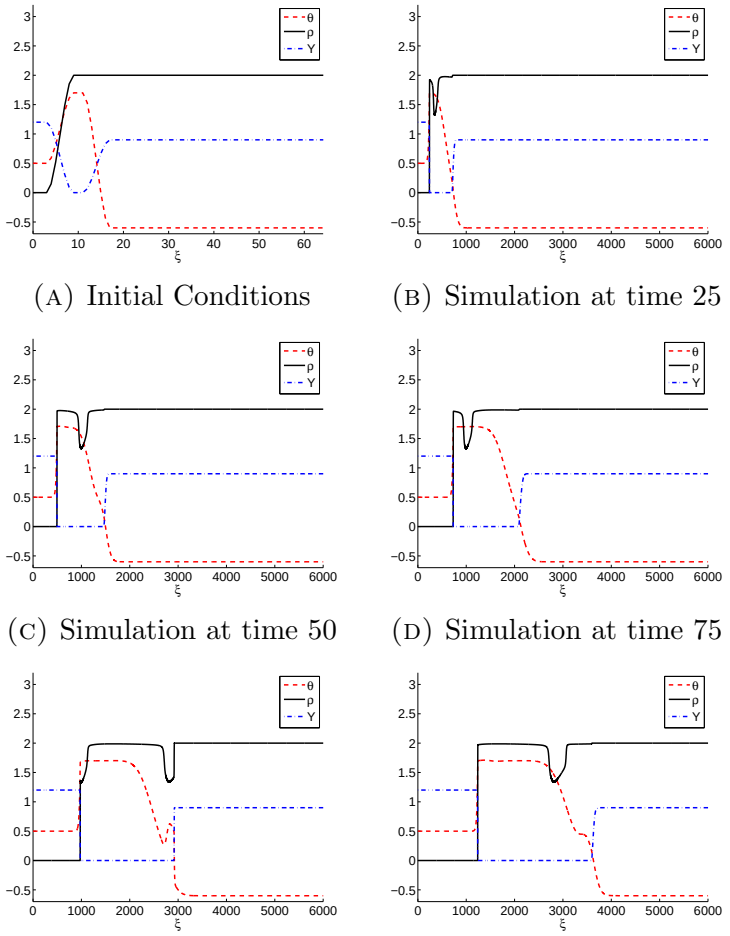

(A) Initial Conditions (B) Simulation at time 25

(C) Simulation at time 50 (D) Simulation at time 75

(E) Simulation at time 100 (F) Simulation at time 125

FIGURE 8.6. Sequence (10); Behavior 1, example 1

data with fast combustion (Sequence (12)) continued to display combustion (Figure 8.14). This is an indication that when $Y^+ > Y^*$, fast combustion of type $FC \xrightarrow{c_f} TC^>$ exists and is stable. In fact, the simulations suggest that when $Y^+ > Y^*$, among (11.1) and (12), the latter is the only stable sequence.

When $Y^+ < Y^*$, three different behaviors were seen, depending on the boundary conditions but not on the type of sequence given as intial condition. Therefore, we will explain the behavior when a sequence of type (11.2) is given as initial condition, noting that the same behavior occurs when a sequence with the same boundary states of type (13) is given as the initial condition. The different behaviors observed mimic those seen in Subsection 8.2.2. Note that sequence (1), which was studied in Subsection 8.2.2, and sequence (13) both have a fast combustion wave of type $OC \xrightarrow{c_f} TC$. The different behaviors are:

(1) The sequence of type (11.2) quickly develops a fast combustion wave of type $OC \xrightarrow{c_f} TC$, hence evolving into sequence (13). The fast combustion wave quickly decreases in magnitude until it becomes imperceptible, at which point the sequence of type (11.2) appears to evolve stably (Figure 8.9).

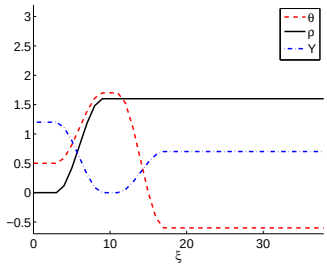

(A) Initial Conditions

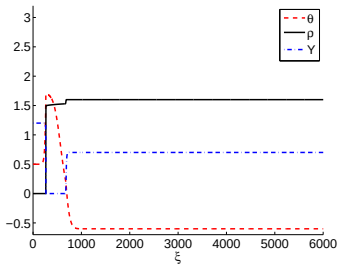

(B) Simulation at time 25

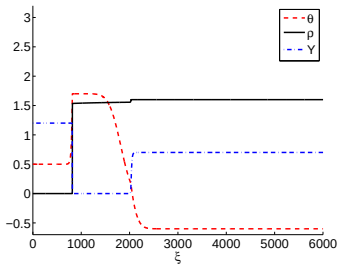

(C) Simulation at time 75

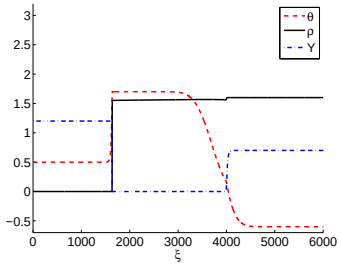

(D) Simulation at time 150

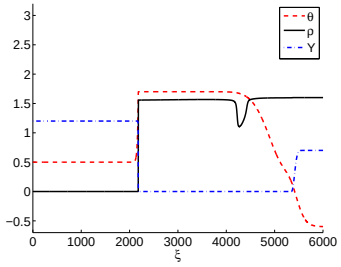

(E) Simulation at time 200

FIGURE 8.7. Sequence (10); Behavior 1, example 2

(2) The sequence of type (11.2) quickly develops a fast combustion wave. The fast combustion wave experiences periodic bursts in magnitude; the period of the bursts increases over time. This behavior is similar to behavior (1) in section 8.2.2 (Figures 8.10 and 8.11).
(3) The sequence of type (11.2) quickly evolves into a sequence of type (13). This sequence then remains stable (Figure 8.12).

The period of the bursts of fast combustion in behavior (2) seems inversely proportional to the magnitude of the sum $\theta^+ + Y^+$). Namely, as $\theta^+ < 0$ decreases and its magnitude approaches the value of Y^+, the period of the bursts decreases. This suggests that, for fixed boundary conditions, there exists a value of θ^+, say $\tilde{\theta}^+$ such that for $\theta^+ < \tilde{\theta}^+$ the sequence will exhibit behavior (1) and for $\theta^+ > \tilde{\theta}^+$ the sequence will exhibit behavior (2).

8.4. **Sequences with boundary conditions** (TC, TC).

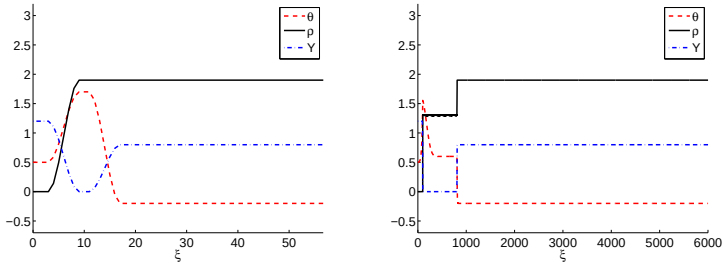

(A) Initial Conditions (B) Simulation at time 10

(C) Simulation at time 25 (D) Simulation at time 50

FIGURE 8.8. Sequence 10; Behavior 2

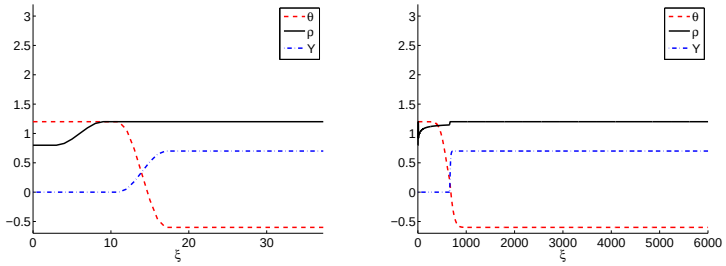

(A) Initial Conditions (B) Simulation at time 25

FIGURE 8.9. Sequence (11.2); Behavior 1

8.4.1. *Sequences of type (14).* The temperature in all wave sequences of type (14) is never positive (i.e., all states in the sequence are of type TC). It is therefore clear that no combustion can occur. It was verified by simulations that all sequences of type (14), namely sequences (14.1)-(14.4.2), are indeed stable.

8.4.2. $S^L \in TC^>, S^R \in TC^<$. The hypotheses of Theorem 3.2 are satisfied but the hypotheses of Theorem 3.1 are not satisfied. Theorem 3.2 shows that slow combustion of type $TC \xrightarrow{cs} OC$ exists. Therefore, it is possible to construct a sequence of type (14.2) and a sequence of type (15.1).

All simulations in which a sequence of type (15.1) was given as initial condition evolved stably. This suggests that sequence (15.1) is indeed stable (see Figure 8.15).

8.4.3. $S^L \in TC^<, S^R \in TC^>$. The hypotheses of Theorem 3.1 are satisfied but the hypotheses of Theorem 3.2 are not satisfied. Theorem 3.1 shows that fast combustion exists.

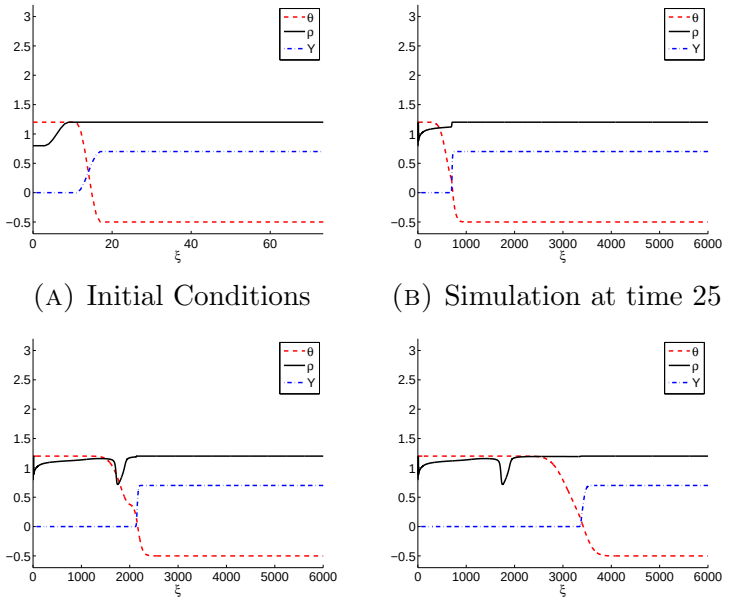

(A) Initial Conditions (B) Simulation at time 25

(C) Simulation at time 75 (D) Simulation at time 125

FIGURE 8.10. Sequence (11.2); Behavior 2, example 1

Furthermore, two types of fast combustion waves are possible: $FC \xrightarrow{c_f} TC$ if $Y^+ > Y^*$ and $OC \xrightarrow{c_f} TC$ if $Y^+ < Y^*$.

If $Y^+ > Y^*$, it is possible to construct a sequence of type (14.3.1) or (16.1).

All simulations in which a sequence of type (16.1) was given as initial condition evolved stably. This suggests that sequence (16.2) is indeed stable (see Figure 8.16).

If $Y^+ < Y^*$, it is possible to construct a sequence of type (14.3.2) or (17.1). Two types of behavior were observed when a sequence of type (17.1) was given as initial condition. If the spacing between the waves was large, the sequence (17.1) evolved stably, so that the fast combustion of type $OC \xrightarrow{c_f} TC$ persisted (see Figure 8.17). If the spacing between the waves is small, the fast combustion wave quickly extinguishes; the sequence evolves into a sequence of type (14.3.2). The extinguishing of the fast combustion wave could possibly be due to the interaction of the low temperature region in the left boundary with the region in which combustion occurs, this interaction being a consequence of diffusion of the heat being generated by the combustion and the heat transported by the contact discontinuity of velocity a (see Figure 8.18).

8.4.4. $S^L, S^R \in TC^>$. The hypotheses of Theorem 3.1 and 3.2 are both satisfied. Theorem 3.2 shows that slow combustion of type $TC \xrightarrow{c_s} OC$ exists. Theorem 3.1 shows that two type of fast combustion wave are possible: $FC \xrightarrow{c_f} TC$ if $Y^+ > Y^*$ and $OC \xrightarrow{c_f} TC$ if $Y^+ < Y^*$.

If $Y^+ > Y^*$, three types of wave sequence are possible: (14.4.1), (15.2), and (16.2). All simulations in which a sequence of type (16.2) was given as initial condition evolved stably. This suggests that sequence (16.2) is indeed stable. The simulations run thus far suggest that sequence (15.2) quickly evolves into a sequence of type (16.2). In other words, when both sequence (15.2) and (16.2) are possible, it appears that sequence (16.2) is stable, whereas sequence (15.2) is unstable.

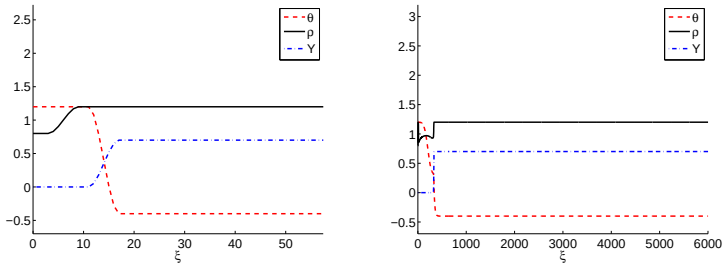

(A) Initial Conditions (B) Simulation at time 10

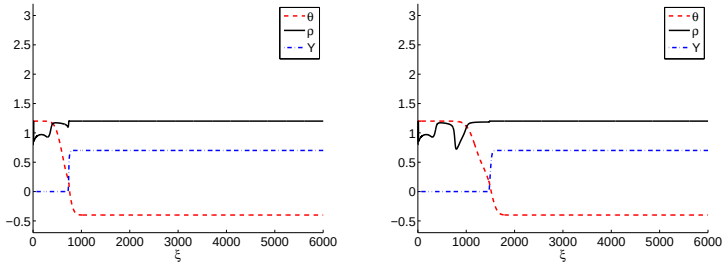

(C) Simulation at time: 25 (D) Simulation at time: 50

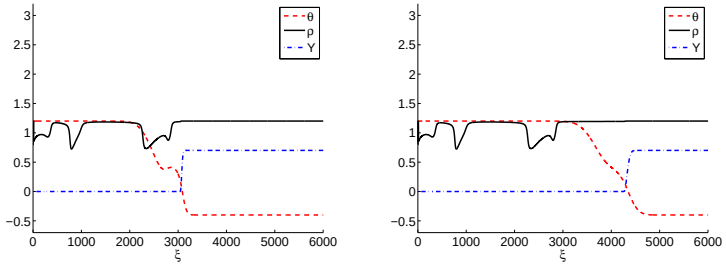

(E) Simulation at time: 100 (F) Simulation at time: 150

FIGURE 8.11. Sequence (11.2); Behavior 2, example 2

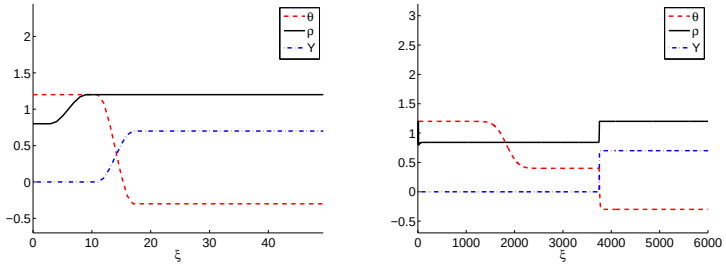

(A) Initial Conditions (B) Simulation at time: 75

FIGURE 8.12. Sequence (11.2); Behavior 3

If $Y^+ < Y^*$, four types of wave sequence are possible: (14.4.2), (15.2), (17.2), and (18).

9. CONCLUSION

The analysis presented in this work leads to the re-classification and re-enumeration of the possible generic wave sequences in the solution of the combustion problem in light porous

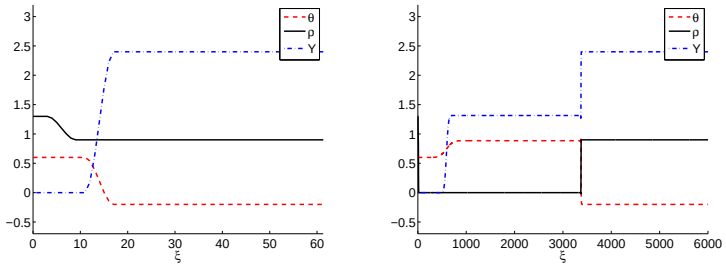

(A) Initial Conditions (B) Simulation at time 25

FIGURE 8.13. Sequence (11.1)

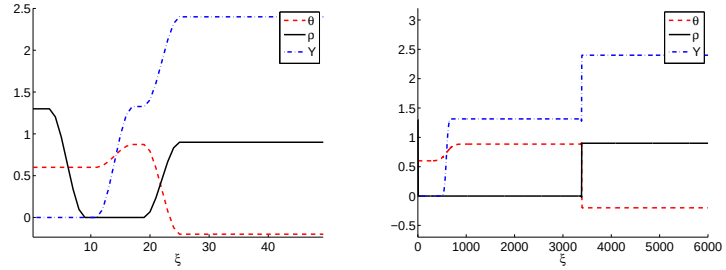

(A) Initial Conditions (B) Simulation at time 25

FIGURE 8.14. Sequence (12)

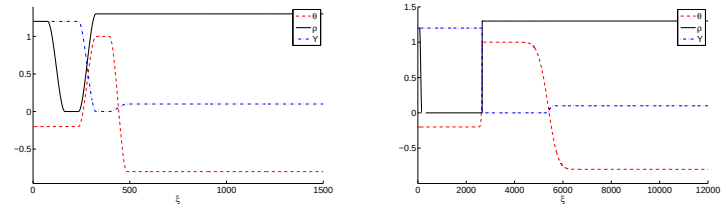

(A) Initial Conditions (B) Simulation at time 200

FIGURE 8.15. Sequence (15.1)

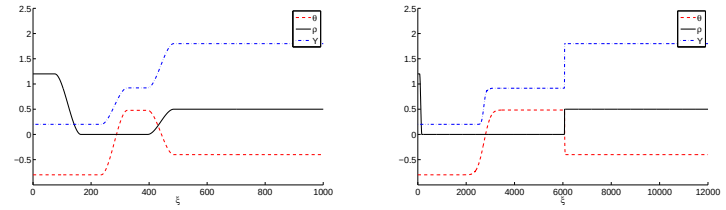

(A) Initial Conditions (B) Simulation at time 200

FIGURE 8.16. Sequence (16.1)

foam. We also studied numerically the hypotheses for existence of the fast combustion waves. This analysis leads to a description of a manifold in parameter space which separates different types of combustion.

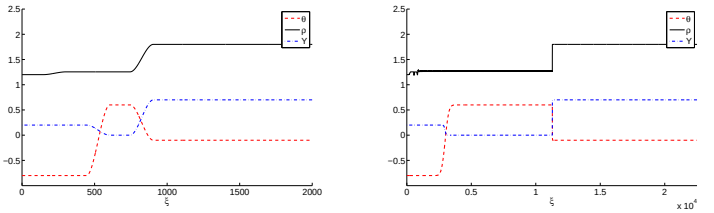

(A) Initial Conditions (B) Simulation at time 100

FIGURE 8.17. Sequence (17.1), large spacing

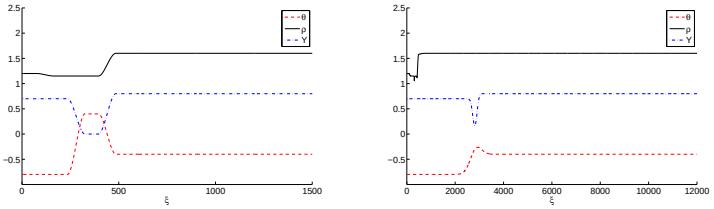

(A) Initial Conditions (B) Simulation at time 100

FIGURE 8.18. Sequence (17.1), small spacing

REFERENCES

[1] I.Y. Akkutlu and Y.C. Yortsos, The dynamics of in-situ combustion fronts in porous media, *J. of Combustion and Flame*, **134** (2003) 229–247.

[2] A.P. Aldushin, I.E. Rumanov, and B.J Matkowsky, Maximal energy accumulation in a superadiabatic filtration combustion wave, *J. of Combustion and Flame*, **118** (1999) 76–90.

[3] A.P Aldushin and B.S Seplyarsky, Propagation of exothermic reaction in a porous-medium during gas blowing, *Sov. Phys. Dokl.*, **23** (1978) 483–485.

[4] J. Bruining, A.A. Mailybaev, and D. Marchesin, Filtration combustion in wet porous medium, *SIAM Journal on Applied Mathematics*, **70** (2009) 1157–1177.

[5] G. Chapiro, *Gas-Solid Combustion in Insulated Porous Media*, Doctoral thesis, IMPA, 2009. http://www.preprint.impa.br.

[6] G. Chapiro, A. A. Mailybaev, A.J. Souza, D. Marchesin, and J. Bruining, Asymptotic approximation of long-time solution for low-temperature filtration combustion, *Comput. Geosciences*, **16** (2012) 799–808.

[7] G. Chapiro, D. Marchesin, S. Schecter, Combustion waves and Riemann solutions in light porous foam, *Journal of Hyperbolic Differential Equations* **11** (2014) 295–328.

[8] J.C. Da Mota and M.M. Santos, An application of the monotone iterative method to a combustion problem in porous media, *Nonlinear Analysis: Real World Applications*, **12(2)** (2011) 1192–1201.

[9] A. Ghazaryan, Y. Latushkin, and S. Schecter, Stability of traveling waves for a class of reaction-diffusion systems that arise in chemical reaction models, *SIAM J. Math. Anal*, **42(6)** (2010) 2434–2472.

[10] A. Ghazaryan, Y. Latushkin, S. Schecter, and A.J. de Souza, Stability of gasless combustion fronts in one-dimensional solids, *Archive for rational mechanics and analysis*, **198(3)** (2010) 981–1030.

[11] C.K.R.T. Jones, Geometric singular perturbation theory in dynamical systems, *Lecture Notes in Math., Springer, Berlin*, **1609** (1995) 44–118.

[12] A.A. Mailybaev, J. Bruining, and D. Marchesin, Analysis of in situ combustion of oil with pyrolysis and vaporization, *Combustion and Flame*, **158(6)** (2011) 1097–1108.

[13] A.A. Mailybaev, D. Marchesin, and J. Bruining, Resonance in low-temperature oxidation waves for porous media, *SIAM Journal on Mathematical Analysis*, **43** (2011) 2230–2252.

[14] D. Marchesin and S. Schecter, Oxidation heat pulses in two-phase expansive flow in porous media, *Zeitschrift für Angewandte Mathematik und Physik (ZAMP)*, **54(1)** (2003) 48–83.

[15] J.C.D. Mota and S. Schecter, Combustion fronts in a porous medium with two layers, *Journal of dynamics and differential equations*, **18(3)** (2006) 615–665.

[16] K. Prasad, R. Kramer, N. Marsh, M. Nyden, T. Ohlemiller, and M. Zammarano, Numerical simulation of fire spread on polyurethane foam slabs, In *Proceedings of the 11th international conference on fire and materials. Interscience Communications, London*, (2009) 697–708.

[17] S. Schecter, The saddle-node separatrix-loop bifurcation, *SIAM journal on mathematical analysis*, **18(4)** (1987) 1142–1156.

[18] S. Schecter and D. Marchesin, Geometric singular perturbation analysis of oxidation heat pulses for two-phase flow in porous media. dedicated to constantine dafermos on his 60th birthday, *Bulletin of the Brazilian Mathematical Society*, **32(3)** (2001) 237–270.

[19] D.A. Schult, B.J. Matkowsky, V.A. Volpert, and A.C. Fernandez-Pello, Forced forward smolder combustion, *Combustion and Flame*, **104(1-2)** (1996) 1–26.

[20] C. Wahle, B. Matkowsky, and A. Aldushin, Effects of gas-solid nonequilibrium in filtration combustion, *Combustion Science and Technology*, **175** (2003) 1389–1499.

[21] Y. B. Zeldovich, G. I. Barenblatt, V. B. Librovich, and G. M. Makhviladze, *The mathematical theory of combustion and explosion*, Consultants Bureau, New York, 1985.